Narrow Linewidth CW Laser Phase Noise Characterization Methods for Coherent Transmission System Applications

Stefano Camatel, *Member, IEEE*, and Valter Ferrero, *Member, IEEE*

***Abstract*—Several techniques for phase noise PSD measurement of continuous wave (CW) lasers to be used in coherent transmission systems are analyzed. Between them, we evaluate two novel techniques. The first employs a homodyne optical phase-locked loop, while the second uses a signal source analyzer. Experimental results obtained by these two methods are compared with classical linewidth measurement methods like self-heterodyne and Michelson interferometer. Limits and accuracy of each method are discussed. Furthermore, the comparison shows that, for coherent transmission system applications, only a subset of the analyzed methods is useful for laser phase noise characterization.**

***Index Terms*—Coherent optical systems, homodyne detection, phase-locked loops, phase measurement, phase noise.**

I. Introduction

RECEIVER sensitivity limit in coherent optical communications is mainly affected by semiconductor laser phase fluctuations [1], [2]. Also, sensors based on optical fiber interferometer systems have a sensitivity limited by phase noise [3]. For these reasons, many works focused on phase noise characteristics of semiconductor lasers have been published [4], [5]. Measurement methods for laser linewidth characterization were proposed in the past years; most of them are based on interferometer techniques [6]–[9].

Here, we analyze several phase noise measurement techniques for testing lasers to be used in optical coherent communications. Common methods based on Michelson interferometer (MI) and delayed self-heterodyne (DSH) measurements are compared with two new techniques. The first novel method [10] is able to retrieve the power spectral density (PSD) of the overall phase noise produced by two lasers, a source laser and a local oscillator (LO) laser. The combined phase noise can then be used for the design and performance estimation of a coherent transmission system. By the way, the CW source laser phase noise PSD could be obtained by this method, if the used LO laser is affected by a negligible phase noise. Our measurement technique is based on an optical phase-locked loop (OPLL) which can be described by a linear model. In this paper, we show experimental results obtained by using an OPLL based on sub-carrier modulation (SC-OPLL) [10]. This way, we are able to characterize CW lasers phase noise; optical oscillators with direct frequency modulation are not required.

The second novel technique is based on a signal source analyzer (SSA) designed for phase noise characterization of radio frequency (RF) oscillators. The optical signal generated by the laser under test is converted into an RF signal through a self-heterodyne architecture; the phase noise of the resulting RF signals is then characterized by a signal source analyzer and postprocessed in order to obtain the PSD of the laser phase noise.

In order to compare the analyzed methods from the experimental point of view, phase noise of two different optical sources has been characterized by using the examined measurement techniques, and the experimental results are presented in this paper.

Section II introduces the notation definitions and expressions needed to describe laser phase noise. The measurement technique based on an OPLL is described in Section III, while Section IV introduces the signal source analyzer method. Section V presents experimental results obtained by using a Michelson interferometer and Section VI shows the linewidth measurements performed through a self-heterodyne technique.

II. Laser Phase Noise Model

The electric field of an unmodulated optical signal emitted by a single-mode semiconductor laser is

$$e(t) = E \cdot \exp\left[j\left(2\pi f_0 t + \phi(t)\right)\right] \tag{1}$$

where E is the amplitude of the electric field and $\phi(t)$ is a random process that represents the phase noise.

Phase noise models usually consider three contributions to the phase noise PSD: white, flicker and random walk noises. The single-sided phase noise PSD $S_\phi(f)$ can then be expressed as

$$S_\phi(f) = \frac{\delta\nu}{\pi f^2} + \frac{k_f}{f^3} + \frac{k_r}{f^4} \tag{2}$$

where $\delta\nu$ is the Lorentzian spectral linewidth of the laser, k_f and k_r are constants that give the strength of flicker frequency noise and random walk frequency noise, respectively.

Manuscript received September 5, 2007; revised March 20, 2008. Current version published December 19, 2008. This work was supported by the BONE-project ("Building the Future Optical Network in Europe"), a Network of Excellence funded by the European Commission through the 7th ICT-Framework Programme, Italian Ministry of University and Research (MIUR), STORiCo Project PRIN 2005.

S. Camatel was with the PhotonLab, Istituto Superiore Mario Boella, 10138 Torino, Italy. He is now with Nokia Siemens Networks (e-mail: stefano.camatel@nsn.com).

V. Ferrero is with the PhotonLab, Dipartimento di Elettronica, Politecnico di Torino, 10129 Torino, Italy (e-mail: valter.ferrero@polito.it).

Digital Object Identifier 10.1109/JLT.2008.925046

The relaxation frequency noise is not taken into account here because it appears at very high frequencies, which are outside the bandwidth of interest for optical coherent transmission systems.

In order to fit the experimental data obtained in the following sections, a nonlinear least squares method was employed. The nonlinear model used for such a fitting is based on a derivation of (2)

$$f(x) = 10 \cdot \log_{10}\left[\frac{\delta\nu}{\pi(10^x)^2} + \frac{k_f}{(10^x)^3} + \frac{k_r}{(10^x)^4}\right] \quad (3)$$

where the function $f(x)$ is the single-sided phase noise PSD measured in dBc and $x = \log_{10}(f)$.

III. OPLL Measurement Method

A. Principle of Operation

The novel measurement technique has been introduced the first time in [10], where the flicker noise and random walk contribution were not kept in account. The operation principle is based on a linear OPLL [see Fig. 1(a)] that can be described by a linear model. An exhaustive study of such a model was presented in [1] and will be used as the starting point of the following treatment. The source laser is not modulated and the phase-lock to data crosstalk will not be taken into account. The signal power level at the OPLL input is set, in order to have shot noise and amplitude electrical noises negligible. This way, the overall phase noise of source and local oscillator lasers is the only contribution that will be considered. The fundamental equation that allows evaluating the phase noise PSD is

$$V_{\mathrm{PL}}(f) = A_{\mathrm{PL}} \cdot \phi_N(f) \cdot [1 - H_{\mathrm{OPLL}}(f)] \quad (4)$$

where $V_{\mathrm{PL}}(f)$ is the Fourier transform of the phase error signal, A_{PL} is a constant coefficient, $\phi_N(f)$ is the phase noise Fourier transform, and $H_{\mathrm{PL}}(f)$ is the PLL closed loop transfer function. A_{PL}, as defined in [1], depends on photodiode responsivity, transimpedance gain, received signal and local oscillator powers. In the experimental setup, shown in Fig. 1(a), the electrical spectrum analyzer (ESA) measures the phase error signal power spectrum $S_{\mathrm{VPL}}(f)$ expressed as

$$S_{\mathrm{VPL}}(f) = A_{\mathrm{PL}}^2 \cdot S_\phi(f) \cdot |1 - H_{\mathrm{OPLL}}(f)|^2 \quad (5)$$

where $S_\phi(f)$ is the phase noise lasers PSD. The $v_{\mathrm{PL}}(t)$ power spectrum is related to the measurement performed by the spectrum analyzer of Fig. 1 through the equation

$$S_{\mathrm{ESA}}(f) = S_{\mathrm{VPL}}(f) \cdot \frac{B_N}{Z_{\mathrm{IN}}} \quad (6)$$

where B_N is the spectrum analyzer noise equivalent bandwidth and Z_{IN} is the spectrum analyzer input impedance.

The PLL transfer function and the constant A_{PL} can be measured in the experimental setup of Fig. 1(b), where the network analyzer returns the following response:

$$G_{\mathrm{NA}}(f) = \frac{\pi^2}{V_\pi^2} A_{\mathrm{PL}}^2 \cdot |1 - H_{\mathrm{OPLL}}(f)|^2 . \quad (7)$$

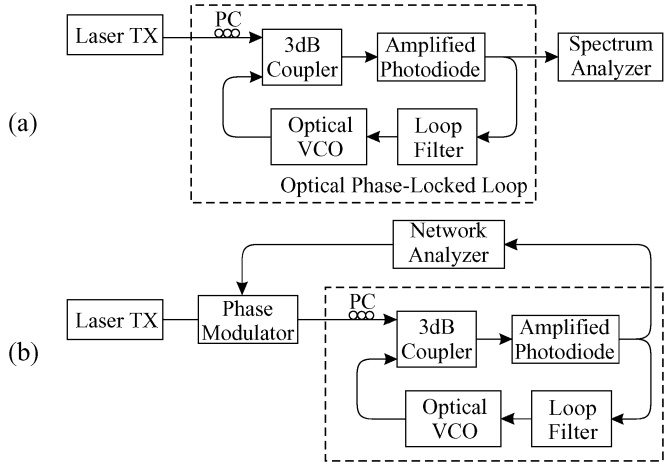

Fig. 1. Setups for measurement of the phase error signal spectrum (a) and the OPLL frequency response (b) necessary for the estimation of the phase noise PSD through the OPLL method.

In (7), V_π is the voltage that has to be applied to the phase modulator in order to get a phase deviation of π radians. From (7), it is possible to calculate the multiplication between the squared constant A_{PL} and the PLL transfer function factor ($|1 - H_{\mathrm{OPLL}}(f)|^2$), which can be substituted in (5) obtaining the following formula:

$$S_{\phi,\mathrm{OPLL}}(f) = \frac{S_{\mathrm{ESA}}(f) \cdot Z_{\mathrm{IN}}}{B_n} \cdot \left[G_{\mathrm{NA}}(f)\frac{V_\pi^2}{\pi^2}\right]^{-1} . \quad (8)$$

Equation (8) returns the PSD of the phase noise lasers given the measurement results obtained by the experiments shown in Fig. 1.

B. Experimental Results

The previously described technique was implemented for the characterization of two couples of external cavity tunable lasers. The first couple includes two Agilent 81640A, while the second couple consists of two Anritsu MG9638A. Declared linewidths are lower than 100 kHz for the Agilent model, and 700 kHz for the Anritsu model. The OPLL employed for phase noise measurement is an SC-OPLL [10]. The signal power at the photodiode input was set to -16 dBm, while the overall LO power was -3 dBm. The photodiode has responsivity equal to 800 V/W. The optical voltage controlled oscillator (VCO) includes a 10-GHz $LiNbO_3$ intensity modulator and a 6-GHz electrical VCO.

For the couple of Agilent 81640A, the loop filter is a first order active filter, whose time constants are $\tau_1 = 3.6$ μs and $\tau_2 = 0.46$ μs. Such time constants were chosen in order to get a second order PLL transfer function with natural frequency $f_0 = 500$ kHz and damping factor $\zeta = 0.707$. The value of $f_0 = 500$ kHz is the lowest natural frequency that allows OPLL locking; thus, it affects the evaluation of $S_\phi(f)$ for low frequency values. Indeed, the $S_\phi(f)$ estimation is accurate as long as the electrical noise power level is negligible with respect to the spectrum $S_{\mathrm{VPL}}(f)$ of the phase error signal. $S_{\mathrm{VPL}}(f)$ usually has a bell-like shape centered around f_0 and the white amplitude noise cannot be neglected for frequency values far from

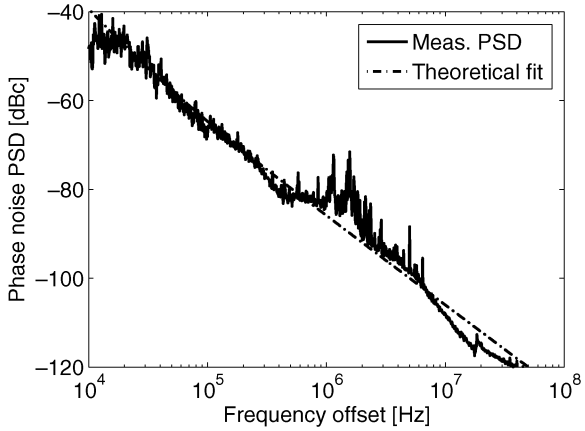

Fig. 2. Measured phase noise PSD of Agilent 81640A tunable laser obtained by OPLL method. A theoretical PSD with $\delta\nu = 7.8$ kHz, $k_f = 9 \cdot 10^7$ Hz^2 and $k_r = 0$ Hz^3 is superimposed.

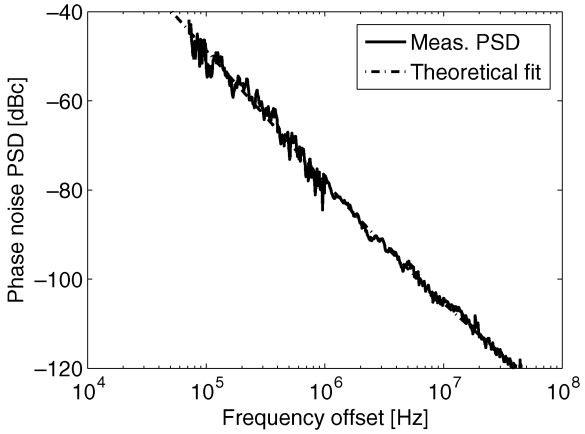

Fig. 3. Measured phase noise PSD of Anritsu MG9638A tunable laser obtained by OPLL method. A theoretical PSD with $\delta\nu = 4.9$ kHz, $k_f = 1.35 \cdot 10^{10}$ Hz^2 and $k_r = 10^6$ Hz^3 is superimposed.

f_0. Therefore, $S_{\mathrm{VPL}}(f)$ cannot be accurately estimated for frequency values much lower or much higher than f_0. Such a fact limits the frequency range on which $S_\phi(f)$ can be correctly evaluated. The upper limit could be overcome by repeating the measurement procedure for higher OPLL natural frequencies. Anyway, the highest OPLL natural frequency that can be set depends on the OPLL loop delay. Our SC-OPLL was affected by a 15-ns feedback loop delay and 8 MHz is the maximum natural frequency for which SC-OPLL can still lock (see [10]). By the way, we were able to measure $S_{\mathrm{VPL}}(f)$ and estimate $S_\phi(f)$ on an acceptable range, so we performed the proposed measurement just with $f_0 = 500$ kHz.

The measurement setups shown in Fig. 1 were performed. The electrical power spectrum was experimentally characterized by the ESA with repeated acquisitions on consecutive frequency intervals. For each frequency interval ESA was set differently: $B_N = 1$ kHz for 10 kHz $< f <$ 100 kHz, $B_N =$ 10 kHz for 100 kHz $< f <$ 1 MHz, $B_N =$ 100 kHz for 1 MHz $< f <$ 10 MHz, and $B_N = 1$ MHz for 10 MHz $< f <$ 100 MHz. Video bandwidth was always set one percent of B_N. The electrical spectrum analyzer of Fig. 1(a) was set with a resolution bandwidth equal to 1 kHz and a video bandwidth of 100 Hz. The network analyzer of Fig. 1(b) generates a signal of 4 dBm and drives a $LiNbO_3$ phase modulator with $\mathrm{V}_\pi = 5$ V. As previously anticipated, the measurements of $\mathrm{S_{ESA}(f)}$ and $\mathrm{G_{NA}(f)}$ allowed the phase noise PSD evaluation of two Agilent 81640A external cavity tunable lasers. Fig. 2 shows the average phase noise PSD of the two Agilent 81640A lasers obtained by half $S_{\phi,\mathrm{OPLL}}(f)$.

A theoretical phase noise PSD $S_\phi(f)$ was computed applying (2); a nonlinear least squares method was applied in order to fit the measured curve of Fig. 2. Due to the limits of such measurement method, previously described, we were not able to take valid experimental data for high values of the phase noise PSD at low frequencies. Experimental data were only taken in a frequency range where random walk noise has not got any significant effect on the measured curve; so we imposed $k_r = 0$ Hz^3. The resulting fitted coefficients were: linewidth $\delta\nu = 7.88$ kHz $\pm 6.2\%$, flicker noise coefficient $k_f = 8 \cdot 10^7 \pm 36\%$ Hz^2. The indicated percentages specify the confidence bounds defined with a 95% level of certainty. The k_f estimate is not as accurate as the linewidth value; a better estimation requires the measurement of the phase noise PSD at lower frequencies.

For the couple of Anritsu MG9638A, the loop filter is still a first order active filter, whose time constants are $\tau_1 = 0.9\ \mu$s and $\tau_2 = 0.23\ \mu$s, corresponding to natural frequency $f_0 = 1$ MHz and damping factor $\zeta = 0.707$. According to the considerations previously made, a higher f_0 was set due to a higher phase noise PSD of the Anritsu lasers at lower frequencies. Fig. 3 shows the average phase noise PSD of the two lasers obtained by half $S_{\phi,\mathrm{OPLL}}(f)$.

Fig. 3 shows also a theoretical phase noise PSD $S_\phi(f)$ computed applying the same procedure previously described, obtaining the linewidth $\delta\nu = 4.9$ kHz $\pm 6.4\%$, the flicker noise coefficient $k_f = 1.35 \cdot 10^{10} \pm 3.6\%$ Hz^2. For the same considerations made for the Agilent laser we imposed $k_r = 0$ Hz^3. With respect to Agilent lasers, the phase noise PSD curve of the Anritsu MG9638A is steeper at low frequencies. Even if Anritsu and Agilent laser are characterized by almost the same amount of white frequency noise, the behavior of the phase noise PSD at low frequencies is much different due to flicker and random walk contributions.

IV. RF Signal Source Analyzer Method

A. Heterodyne Characterization

This method is based on the characterization of the electrical signal obtained by the beating of two laser signals. Phase noise characterization should actually be performed by RF instruments designed for the analysis of electrical signal sources. Actually, lasers are less stable in frequency than RF sources; so we excluded the use of instruments whose measurement is based on a simple electrical phase locked loop which fails to measure phase noise of relatively drifty and noisy signal sources. We tried to use an Agilent E5052 which employs a heterodyne discriminator method in order to measure relatively large phase noise of unstable signal sources. Even if such instrument is more tolerant to frequency drifting signals, it was not able measure lasers phase noise. Thus, we will not present

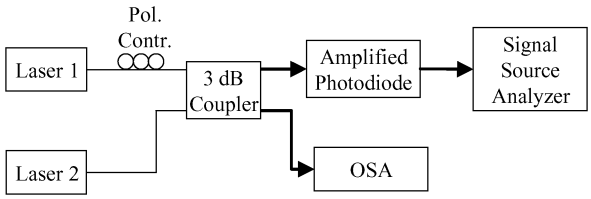

Fig. 4. Heterodyne setup for the measurement of the combined phase noise PSD of two lasers based on a signal source analyzer.Narrow Linewidth CW Laser Phase Noise Characterization Methods for Coherent

any measurement result got with this method but its description is useful in order to understand the next measurement method.

The experimental setup is illustrated in Fig. 4: both lasers are tuned appropriately and their optical frequencies are kept constant during the measurement. The polarization controller is used to align lasers' polarization state at the photodetector input. The coupler combines the two optical fields, obtaining half inputs total power to each output port. The upper output port is connected to a photodiode that detects the interference beat tone between the two lasers, converting it into an electrical tone. Note that lasers frequency must be tuned in order to have the mixing product in the photodetector and signal source analyzer electrical bandwidth. The lasers wavelength tuning operation is monitored by using an OSA. The resulting heterodyne beat signal is described by

$$v_{\mathrm{PL}}(t) = 2R\sqrt{P_1 P_2}\cos\left(2\pi(f_1 - f_2)t + \Delta\phi(t)\right) \quad (9)$$

where the resulting phase noise is given by

$$\Delta\phi(t) = \phi_1(t) - \phi_2(t). \quad (10)$$

The resulting signal is a sine wave in the RF domain where the overall electrical phase noise $\Delta\Phi(\mathrm{t})$ is due to the lasers optical phase noise contributions. Such a electrical noise can be characterized employing the phase noise PSD measurement techniques for RF oscillators, i.e. by using a RF signal source analyzer. Actually such a measurement returns the overall phase noise generated by both lasers of Fig. 4 being the two processes $\phi_1(\mathrm{t})$ and $\phi_2(\mathrm{t})$ uncorrelated. If we are interested in laser 1 phase noise PSD contribution only, it could be evaluated employing a laser 2 (Local Oscillator) with phase noise PSD negligible with respect to the one of laser 1, so the resulting phase noise may be approximated as $\Delta\phi(t) \approx \phi_1(t)$.

The experimental setup was built using an Agilent E5052 signal source analyzer. Such instrument is able to characterize the phase noise of RF signals if oscillator frequency is sufficiently stable. In fact, it is able to track frequency variations in a range lower than 3 MHz. Unfortunately, frequency stability of the heterodyne beat signal was much worse; the instrument was not able to track the input signal and measurement could not be performed.

In order to solve the problem of frequency stability, the experimental setup of Fig. 4 was modified and a self-heterodyne measurement was performed as described in the following section.

B. Correlated Delayed Self-Heterodyne Characterization

This method is obtained by substituting the heterodyne architecture of Fig. 4 with the delayed self-heterodyne one as shown in Fig. 5. Correlated delayed self-heterodyne technique employs just one laser for RF beat signal generation. The optical source signal is split into two paths by the first splitter. The optical frequency of one arm is offset with respect to the other of δf. Unlike the traditional delayed self-heterodyne technique described in Section VI, here the delay τ of one path must be much lower than the coherence time of the source laser in order to solve the frequency instability problem that affects the previously described method. Thus, the two combining beams are not statistically independent. The beat tone produced is displaced from 0 Hz to δf thanks to the frequency shift. A signal source analyzer measures the RF beat tone phase noise PSD, which is broadened by the laser linewidth. Actually, phase noise information is translated from optical frequencies to RF frequencies where electronics instrumentation operates.

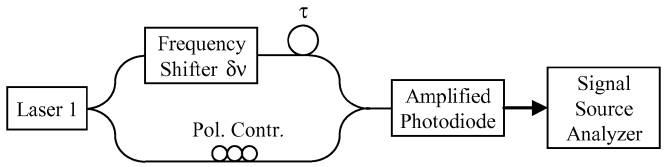

Fig. 5. Delayed self-heterodyne setup for the phase noise PSD measurement of a laser based on a signal source analyzer.

The signal at the photodetector output is given by

$$v_{\mathrm{PL}}(t) = \frac{\mathrm{R}P_S}{2}\left[1+\cos\left(2\pi\delta f t + 2\pi(f_S+\delta f)\tau + \Delta\phi(t,\tau)\right)\right] \quad (11)$$

where the resulting phase noise is given by

$$\Delta\phi(t,\tau) = \phi_S(t+\tau) - \phi_S(t). \quad (12)$$

Note that (11) does not include any term regarding the phase noise introduced by the frequency shifter. Since the laser phase noise is much higher than the electrical oscillator in the frequency shifter, this assumption is easily satisfied. Anyway, the amplitude of $\Delta\phi(t,\tau)$ is lower as delay τ decreases and τ can not be set to too small values.

From (12), the relation between the Fourier transforms of $\Delta\phi(t,\tau)$ and $\phi(t)$ is derived as

$$\Delta\Phi(f) = \Phi(f)\cdot\left[1 - e^{-j2\pi f\tau}\right]. \quad (13)$$

A signal source analyzer characterizes the phase noise PSD $S_{\Delta\phi}(f)$. The phase noise PSD $S_\phi(f)$ is related to the measured $S_{\Delta\phi}(f)$ by the following equation:

$$S_{\phi,\mathrm{SSA}}(f) = \frac{S_{\Delta\phi}(f)}{\left|1 - e^{-j2\pi f\tau}\right|^2} = S_{\Delta\phi}(f)\cdot\frac{1}{4\sin^2(\pi f\tau)}. \quad (14)$$

In order to verify the right setting of the delay τ, the measured $S_{\Delta\phi}(f)$ must be much higher than the signal phase noise PSD used for the frequency shifter operations

The experimental setup of Fig. 5 was built using an acousto-optic modulator driven by a 27-MHz electrical oscillator. An Agilent E5052 signal source analyzer characterized the electrical signal phase noise PSD. The delay τ was set to 6 ns. By using the measured $S_{\Delta\phi}(f)$, laser phase noise PSD was computed by (14). The Agilent 81640A tunable laser was characterized and the result is plotted in Fig. 6. A fitting curve was

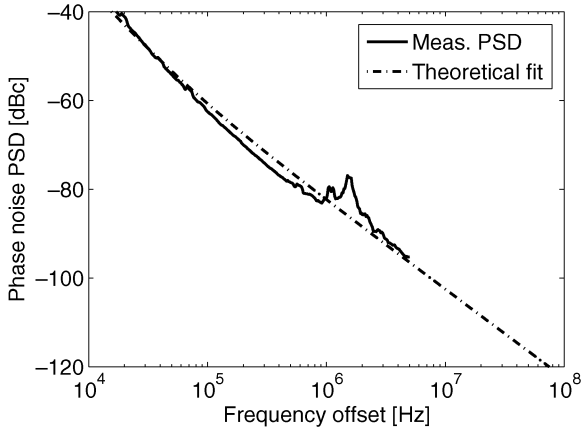

Fig. 6. Measured phase noise PSD of Agilent 81640A tunable laser obtained by DSH signal source analyzer method. A theoretical PSD with $\delta\nu = 17.5$ kHz, $\mathrm{k_f} = 2.9 \cdot 10^8$ Hz^2 and $\mathrm{k_r} = 0$ Hz^3 is superimposed.

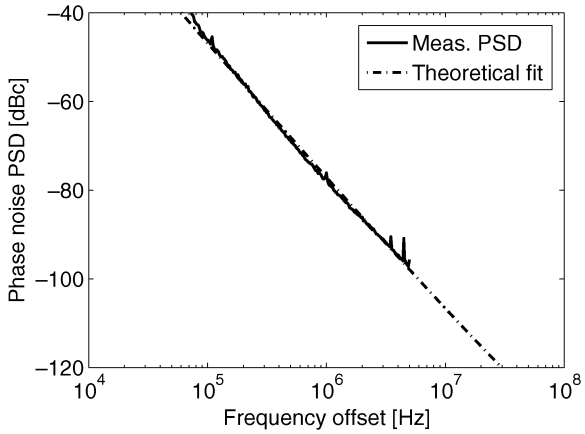

Fig. 7. Measured phase noise PSD of Anritsu MG9638A tunable laser obtained by DSH signal source analyzer method. A theoretical PSD with $\delta\nu = 807$ Hz, $k_f = 1.9 \cdot 10^{10}$ Hz^2 and $k_r = 1.5 \cdot 10^{14}$ Hz^3 is superimposed.

computed for a theoretical phase noise PSD characterized by a linewidth $\delta\nu = 17.5$ kHz $\pm 9\%$, a flicker noise coefficient $k_f = 2.9 \cdot 10^8 \pm 16\%$ Hz^2. The random walk coefficient k_r was imposed to be zero because the experimental data were taken in a frequency range where random walk noise has not got any effect. The SSA returned experimental data only for frequencies up to 5 MHz, where the phase noise PSD behave differently from a white frequency noise; so we believe that the linewidth is overestimated.

Fig. 7 shows the measurement of the Anritsu MG9638A, and the resulting phase noise PSD parameters are $\delta\nu = 1.4$ kHz $\pm$ 100%, a flicker noise coefficient $k_f = 1.9 \cdot 10^{10} \pm 5.2\%$ Hz^2 and a random walk coefficient $k_r = 1.5 \cdot 10^{14} \pm 13.2\%$ Hz^3. Also in this case, linewidth estimation is not accurate because it requires experimental data at frequencies higher than 5 MHz.

V. Michelson Interferometer Method

A Michelson interferometer is sometimes used for the laser phase noise characterization. Actually it is a frequency discriminator which converts optical carrier fluctuations into intensity variations that can be directly measured. The experimental setup is shown in Fig. 8. The laser under test is followed by an isolator

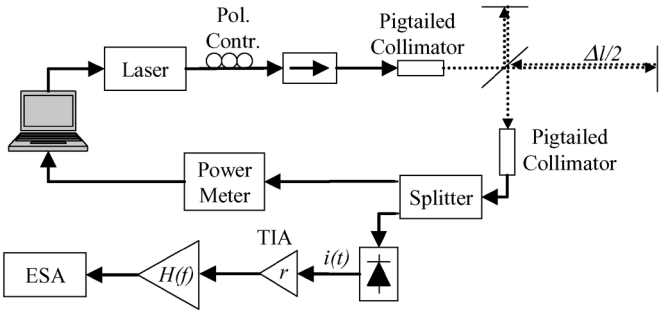

Fig. 8. Setup for the phase noise PSD measurement based on the Michelson interferomenter method.

in order to avoid that undesired reflections into the laser coming back from the interferometer induce instabilities. The main parameter that characterizes this type of discriminator is the differential optical time delay τ between the two paths through the interferometer. The output from the interferometer is detected by an amplified PIN photodiode. The PSD of the resulting electrical signal is measured by a spectrum analyzer. Part of the optical power from the interferometer is measured by a power monitor. A routine running on the PC reads the power level and controls the laser radiation wavelength in order to keep it locked to the interferometer characteristic.

The phase noise spectrum is related to the interference signal spectrum in the following way. The PIN photodiode output, neglecting intensity noise, is

$$i(t) = i_0 + \Delta i \cdot \cos\left(2\pi f_0 \tau + \Delta\phi(t,\tau)\right) \tag{15}$$

$$\Delta\phi(t,\tau) = \phi(t+\tau) - \phi(t) \tag{16}$$

where i_0 is the mean value of the current, Δi is equal to the maximum amplitude of the photocurrent variations due to optical interference, and $\tau = \Delta l/c$ where Δl is the optical path-length difference.

This method requires the interferometer to be adjusted in quadrature; thus, f_0 must be chosen in order to satisfy the condition $2f_0\tau = n + 1/2$ for any positive integer n. Moreover, choosing τ small enough, we assume that $\Delta\phi(t,\tau) \ll 1$ and $\sin[\Delta\phi(t,\tau)] \approx \Delta\phi(t,\tau)$; thus, (15) becomes

$$i(t) = i_0 + (-1)^n \Delta i \cdot \Delta\phi(t,\tau). \tag{17}$$

Therefore, we can determine the phase difference spectrum $S_{\Delta\phi}(f)$ induced in the delay time τ, from the spectrum $S_i(f)$ of the fluctuating current by

$$S_{\Delta\phi}(f) = S_i(f)/\Delta i^2. \tag{18}$$

The spectrum of $i(t)$ is related to the measurement performed by the spectrum analyzer of Fig. 8 through the equation

$$S_{\mathrm{ESA}}(f) = S_i(f) \cdot r^2 \cdot |H(f)|^2 \cdot \frac{B_N}{Z_{\mathrm{IN}}} \tag{19}$$

where r is the TIA transimpedance gain, $H(f)$ is the low noise amplifier transfer function, B_N is the spectrum analyzer noise equivalent bandwidth and Z_{IN} is the spectrum analyzer input impedance.

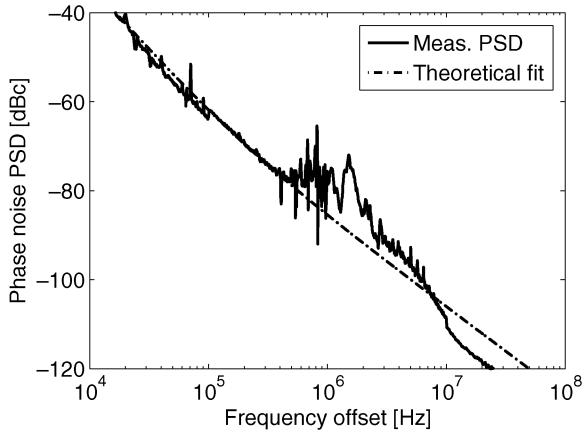

Fig. 9. Measured phase noise PSD of Agilent 81640A tunable laser obtained by Michelson interferometer method. A theoretical PSD with $\delta\nu = 7.7$ kHz, $\mathrm{k_f} = 4.1 \cdot 10^8$ Hz^2 and $\mathrm{k_r} = 0$ Hz^3 is superimposed.

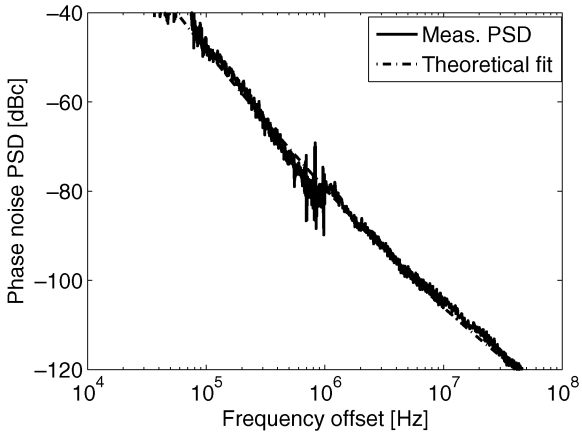

Fig. 10. Measured phase noise PSD of Anritsu MG9638A tunable laser obtained by Michelson interferometer method. A theoretical PSD with $\delta\nu = 4.7$ kHz, $k_f = 9.8 \cdot 10^9$ Hz^2 and $k_r = 4.5 \cdot 10^{14}$ Hz^3 is superimposed.

The relation (13), introduced in the previous section, between the $\Delta\phi(t,\tau)$ Fourier transforms and $\phi(t)$, is still valid in this case. Therefore, by using (14), (18), and (19), the phase noise PSD of the laser under test is computed by

$$S_{\phi,\mathrm{MI}}(f) = \frac{1}{4\sin^2(\pi f\tau)} \cdot \frac{Z_{\mathrm{IN}}}{\Delta i^2 \cdot B_N \cdot r^2 \cdot |H(f)|^2} \cdot S_{\mathrm{ESA}}(f). \tag{20}$$

The experimental setup shown in Fig. 8 was used to measure the phase noise PSD of the Agilent 81640 tunable laser. The FM discriminator time delay was measured using a lightwave component analyzer. By measuring the interferometer optical intensity modulation transmission characteristic versus the modulation frequency, a sinusoidal pattern with 1.43-GHz period was obtained. Since the interferometer differential time delay is equal to the inverse of such period, we got $\tau = 0.7$ ns. Next, the photocurrent peak-to-peak variation due to the interference was measured by tuning the laser, measuring $\Delta i = 4$ mA. The transimpedance amplifier gain and the ESA input impedance were respectively $r = 1\ \mathrm{k}\Omega$ and $Z_{\mathrm{IN}} = 50\ \Omega$. Several spectrum analyzer resolution bandwidths were set depending on the frequency range the measurements had to be performed: $B_N = 1$ kHz for 10 kHz $< f <$ 100 kHz, $B_N = 10$ kHz for 100 kHz $< f <$ 1 MHz, $B_N = 100$ kHz for 1 MHz $< f <$ 10 MHz, and $B_N = 1$ MHz for 10 MHz $< f <$ 100 MHz.

Fig. 9 shows $S_\phi(f)$ against f for the Agilent 81640A tunable laser. Measured curve was unstable because the control loop was not able to completely compensate for interferometer instabilities caused by vibrations. Measurements based on this method are very sensitive to external interferences and requires a fast feedback circuit.

Fig. 9 shows also the fitting curve that was computed for a theoretical phase noise PSD characterized by a linewidth $\delta\nu = 8.3$ kHz $\pm\ 5.5\%$, a flicker noise coefficient $k_f = 3.9 \cdot 10^8 \pm 9.3\%$ Hz^2. Random walk coefficient k_r was imposed to be zero for the same reasons described above. Fig. 10 shows $S_\phi(f)$ characterization for Anritsu MG9638A and the fitting theoretical phase noise PSD with parameters linewidth $\delta\nu = 4.7\,\mathrm{kHz}\pm5\%$, flicker noise coefficient $k_f = 9.8 \cdot 10^9 \pm 4.9\%$ Hz^2 and random walk coefficient $k_r = 4.5 \cdot 10^{14} \pm 10.1\%$ Hz^3.

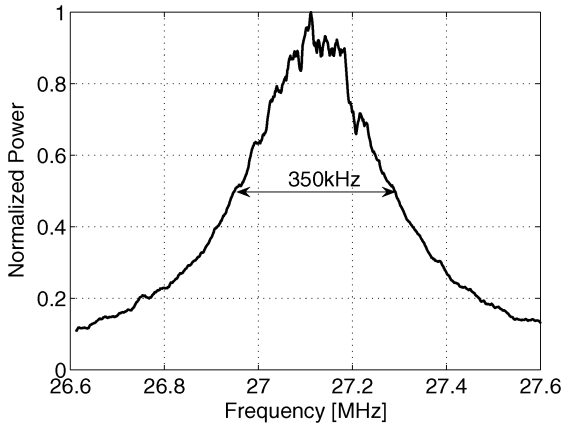

Fig. 11. Delayed self-heterodyne measurement results for Agilent 81640A tunable laser, which show $\delta\nu = \mathrm{FWHM}/2 = 175$ kHz.

VI. Self-Heterodyne Method

Both Agilent and Anritsu lasers were characterized by a delayed self-heterodyne measurement technique [11]. With respect to the method base on a signal source analyzer of Section IV-B, such a measurement setup requires the recombination of two optical field replica, that must be uncorrelated each other by means of an appropriate delay. Therefore, a 20 km spoon fiber was used as delay line. An acousto-optic modulator was also used to perform a 27 MHz frequency shift. Figs. 11 and 12 show the detected spectra, which reveal a linewidth of almost 175 kHz for the Agilent 81640A and 600 kHz for the Anritsu MG9638A laser.

Such measurement technique gave different results with respect to the measurement methods previously described. This fact was just observed in [6] during the characterization of DFB lasers and is due to an overestimation of the linewidth when the self-heterodyne method have to deal with deviations of the laser lineshape from the Lorentzian shape, i.e. when the frequency noise spectrum is no longer a flat spectrum because of f^{-n} terms. Such f^{-n} contributions correspond to optical frequency instability and usually have very low speed variation. From an empirical point of view, it can be explained by a frequency shifting, varying with time, of a perfect Lorentzian shape (see

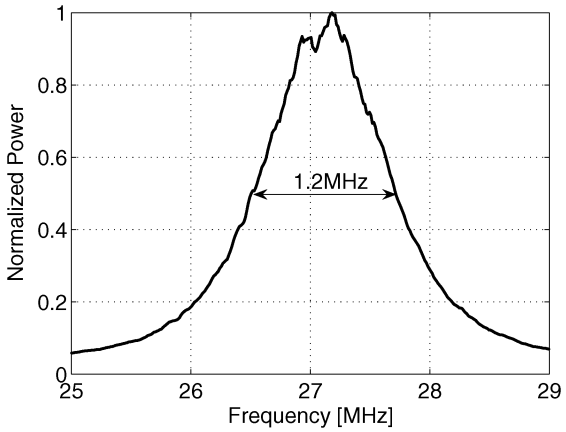

Fig. 12. Delayed self-heterodyne measurement results for Anritsu MG9638A tunable laser, which show $\delta\nu = \mathrm{FWHM}/2 = 600$ kHz.

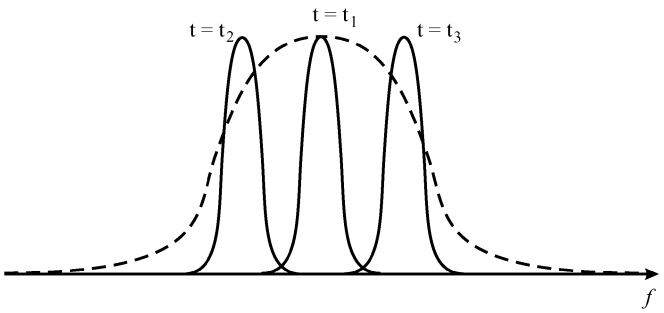

Fig. 13. Instantaneous shots of the drifting Lorentzian spectrum (straight lines) varying with time and long term spectrum (dotted) obtained by a protracted observation.

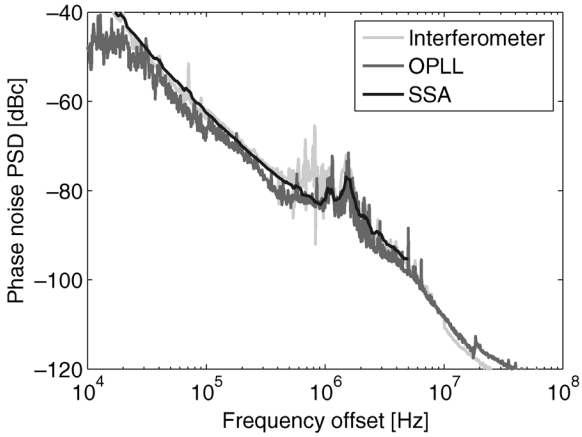

Fig. 14. Measured phase noise PSD of Agilent 81640A tunable laser obtained by OPLL, signal source analyzer and interferometer methods.

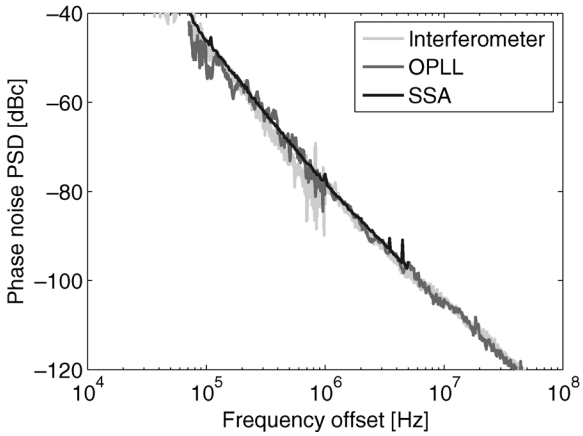

Fig. 15. Measured phase noise PSD of Anritsu MG9638A tunable laser obtained by OPLL, signal source analyzer and interferometer methods.

Fig. 13). The self heterodyne (or also self homodyne) method, due to a low speed measurement and large delay time (higher than laser coherence time), is able to measure only the envelope of the frequency drifting "perfect" Lorentzian source (see Fig. 13).

Since the other measurement techniques analyze phase noise contributions for every spectral component, it is possible to calculate the overall phase noise amount on the limited frequency range where the coherent optical receiver operates. Note that, normally the coherent optical receiver does not take into account f^{-n} contributions at low frequencies. Such low-frequency contributions are not ignored in the self-heterodyne measurement, but they do not affect performance in coherent systems applications, so they do not have to be considered in laser phase noise experimental characterizations. For this reason, the other methods are more reliable for coherent communications because they estimate the "correct" amount of noise that affect the performance. The self heterodyne and self homodyne mentioned methods overestimate the phase noise amount for coherent applications.

VII. Discussion

For the reasons discussed before, the self heterodyne and self homodyne techniques (Section VI) overestimate the phase noise amount for the coherent applications point of view. Figs. 14 and 15 show the curves measured by OPLL, signal source analyzer and interferometer method. The comparison demonstrates a very good agreement in terms of experimental results for both Agilent and Anritsu Laser characterizations. This demonstrates the validity of the introduced novel methods.

Note that the Michelson interferometer method (Section V) is very sensitive to external interferences and requires a fast feedback circuit; indeed, if the control loop is not able to completely compensate the interferometer instabilities caused by vibrations, the measured curve becomes unstable.

The RF signal analyzer method (Section IV), due to the laser wavelength instabilities, can be applied using only the self heterodyne setup (Fig. 5). It requires a very accurate measurement of the time delay τ, being the measurement result strongly dependent on such value.

Finally, the novel method based on SC-OPLL (Section III) is as accurate as RF signal source analyzer method (Section IV), without using any fiber spool. It is sensitive to the loop filter parameters, but they can be easily changed and, in theory, it is possible to implement an automatic procedure to optimize loop filter parameters for every measurement.

VIII. Conclusion

An analysis of several techniques for the acquisition of the laser phase noise PSD has been performed. Novel measurement

methods have been compared with commonly used techniques. Two tunable lasers have been characterized and measurement results obtained by applying all the methods were compared. Experiments able to retrieve the phase noise PSD returned similar results and characteristics of each method have been discussed. Furthermore, we demonstrated that other approaches, such as delayed self-heterodyne, give a pessimistic estimation of the linewidth. Thus, only a subset of the analyzed methods is useful for the laser optical phase noise characterization for the coherent applications point of view. Therefore, the proposed novel techniques give an accurate linewidth estimation to be used in the performance evaluation and design of coherent optical transmission systems.

REFERENCES

[1] L. G. Kazovsky, "Balanced phase-locked loops for optical homodyne receivers: Performance analysis, design considerations, and laser linewidth requirements," *J. Lightw. Technol.*, vol. 4, no. 2, pp. 182–195, Feb. 1986.

[2] S. Norimatsu and O. Ishida, "Impact of flicker noise and random-walk noise on a phase-locked loop with finite propagation delay," *J. Lightw. Technol.*, vol. 12, no. 1, pp. 86–95, Jan. 1994.

[3] A. Dandridge and A. B. Tveten, "Phase noise of single-mode diode lasers in interferometer systems," *Appl. Phys. Lett.*, vol. 39, p. 530, 1981.

[4] B. Daino, P. Spano, M. Tamburrini, and S. Piazzolla, "Phase noise and spectral line shape in semiconductor lasers," *IEEE J. Quant. Electron.*, vol. QE-19, no. 3, pp. 266–270, Mar. 1983.

[5] C. H. Henry, "Phase noise in semiconductor lasers," *J. Lightw. Technol.*, vol. T-4, no. 3, pp. 298–311, Mar. 1986.

[6] M. O. van Deventer, P. Spano, and S. K. Nielsen, "Comparison of DFB laser linewidth measurement techniques results from COST 215 round robin," *Electron. Lett.*, vol. 26, pp. 2018–2020, 1990.

[7] T. Okoshi and K. Kikuchi, *Coherent Optical Fiber Communications*. New York: Kluwer, 1988.

[8] S. Piazzolla, P. Spano, and M. Tamburrini, "Characterization of phase noise in semiconductor lasers," *Appl. Phys. Lett.*, vol. 41, p. 695, 1982.

[9] O. Ishida, "Delayed-self-heterodyne measurement of laser frequency fluctuations," *J. Lightw. Technol.*, vol. 9, no. 11, pp. 1528–1533, Nov. 1991.

[10] S. Camatel and V. Ferrero, "Phase noise power spectral density measurement of narrow linewidth CW lasers using an optical phase-locked loop," *IEEE Photon. Technol. Lett.*, vol. 18, no. 23, pp. 2529–2531, Dec. 2006.

[11] T. Okoshi, K. Kikuchi, and A. Nakayama, "Novel method for high resolution measurement of laser output spectrum," *Electron. Lett.*, vol. 16, p. 630, 1980.

Stefano Camatel (M'04) received the Laurea degree in electronic engineering (summa cum laude) in 2001 and the Ph.D. degree in electronic and communication engineering in 2005, both from the Politecnico di Torino, Torino, Italy.

From June 2003 to June 2004, he was a visiting researcher at the University of California, Santa Barbara (UCSB). In 2005, he was a Postdoctorate at the Politecnico di Torino, working on new modulation formats for next-generation optical networks. From 2006 to 2008, he was a researcher at the Istituto Superiore Mario Boella working on free space optical communications, coherent detection, and plastic optical fibre communication systems. He is currently with Nokia Siemens Networks.

Valter Ferrero (M'97) received the Laurea degree (summa cum laude) in ingegneria elettronica from the Politecnico di Torino, Torino, Italy, in 1994.

In 1994, he collaborated with the Politecnico di Torino, working on optical coherent systems. From 1995 to 1996, he was with GEC Marconi, Genova, Italy. In 1997, he was in charge of the optical laboratory, Department of Electrical Engineering, Politecnico di Torino, and was promoted to Assistant Professor in 2001. He is currently with the Optical Communication Group, Politecnico di Torino, supervising the PhotonLab optical laboratory conduction and directing several research projects related to optical communications. His current research interests include optical coherent communications and free-space optical communications.